Available online at www.sciencedirect.com
SCIENCE DIRECT®
Carbohydrate Polymers 53 (2003) 241–252
Carbohydrate Polymers
www.elsevier.com/locate/carbpol

Structural features and potential texturising properties of lemon and maize cellulose microfibrils

C. Rondeau-Mouro[a,*], B. Bouchet[b], B. Pontoire[a], P. Robert[a], J. Mazoyer[c], A. Buléon[a]

[a]*Unité de Physico-Chimie des Macromolécules, Institut National de la Recherche Agronomique, Rue de la Géraudiere BP 71627, 44316 Nantes Cedex 03, France*
[b]*Unité de Recherches sur les Parois, leurs Interactions et leurs Organisations, Institut National de la Recherche Agronomique, Rue de la Géraudière BP 71627, 44316 Nantes Cedex 03, France*
[c]*Degussa, Centre de Recherches de Baupte-50100 Carentan, France*

Received 6 June 2002; revised 19 September 2002; accepted 30 September 2002

Abstract

Cellulose microfibrils extracted from lemon and maize were studied by solid state NMR, Wide Angle X-ray Scattering, Fourier Transform Infrared Spectroscopy and Transmission Electron Microscopy. Some structural characteristics such as the allomorphic composition, the degree of crystallinity and the lateral or longitudinal crystal size were determined. These depended on the processing conditions, especially grinding, and determined the texturising properties of the microfibrils for liquid food product. Hydrolysed tunicin and Avicel were also studied as reference systems in terms of crystallinity and texturising properties in water. Lemon cellulose was shown to have a higher crystallinity or crystal size and a better texturising behaviour than maize microfibrils. Nevertheless, lemon microfibrils are more sensitive to grinding which decreases systematically the crystallinity and increases the amount of Iβ allomorph. Solid state NMR was also used to probe the mobility of the different regions of microfibrils by measuring $T_{1\rho}$ which was well correlated to crystallinity. The presence of both surface and internal amorphous areas was discussed with respect to the NMR and X-ray scattering data. Some possible hypotheses for discrepancies observed between lemon and maize microfibrils in terms of texturising properties are expressed. Finally, these various properties were studied in the presence of polysaccharides such as carboxymethyl cellulose, scleroglucan or xanthan.

Keywords: Structure; Cellulose microfibrils; Lemon; Maize; Texturising properties

1. Introduction

Cellulose is the most common organic substance in nature. It is not only present in plants, but also in bacteria, fungi, algae and even in animals (in tunicates for instance) (Atalla, 1999; Horii, 2000; Salmon & Hudson, 1997). Cellulose is produced by higher plants (wood, cotton, flax, hemp or ramie), and is localised in the cell-wall, forming a network of linear 'bundles' called microfibrils embedded in a non-cellulosic matrix constituted of polysaccharides (pectins and hemicelluloses) and small amounts of proteins and polyphenolic molecules. The role and properties of each cell-wall constituent are not fully understood but some of them interact with cellulose in order to maintain the structure and the architecture of cell walls, whereas the pectic polysaccharides form a tri-dimensional network, trapping water resulting in a type of gel (Carpita & Gibeaut, 1993; Sarko, 1978). In addition to its enormous commercial value in paper, textile and wood products, cellulose is also present in many waste products of the agro-industries such as sugar and fruit juice processing and also pectin extraction from fruits (Dinand, Chanzy, & Vignon, 1996). Cellulosic microfibrils can be extracted from these by-products traditionally used for cattle feed and processed as food or cosmetic additives for their gelling and thickening properties in water (Dinand, Chanzy, & Vignon, 1999). Some cellulosic products such as the colloidal microcrystalline cellulose (MCC) are already available on the market as food additives used for stabilisation (Ginley & Tauson, 1990). Once dispersed, the solid particles interact between themselves in order to build up a network which provides a gel structure to the aqueous medium. Thus some cellulosic products, like colloidal MCC, when properly dispersed, are able to provide interesting stabilising

* Corresponding author. Tel.: +33-240-6750-50; fax: +33-240-6750-43.
E-mail address: rondeau@nantes.inra.fr (C. Rondeau-Mouro).

0144-8617/03/$ - see front matter © 2003 Elsevier Science Ltd. All rights reserved.
doi:10.1016/S0144-8617(03)00069-9

properties at low concentrations (Nussinovitch, 1997). The dispersion level is dependent on the composition of the aqueous solvent, if salts or acids are present then complete particle dispersion is more difficult. Protective hydrocolloïds such as carboxymethyl cellulose (CMC) or xanthan can be added within the cellulose production stages to ensure easier dispersion. In addition, the origin of cellulose and some production parameters may also affect its dispersion. The mechanical characteristics of cellulose microfibrils from sugar beet pulps (Dufresne, Cavaillé, & Vignon, 1997) and potato tuber cells (Dufresne, Dupeyre, & Vignon, 2000) were studied, the latter being incorporated in starch cellulose-composites.

Among the numerous methods used to investigate properties of the cellulose, X-ray crystallography provides direct information about structure. The polymorphism of cellulose was established relatively early (Davis, Barry, Peterson, & King, 1943; Hess & Kiessig, 1941; Petitpas, Oberlin, & Mering, 1963; Sarko & Mugli, 1974) and apart from the native cellulose I, five other crystalline forms labelled II, III_I, III_{II}, IV_I and IV_{II} are now well-known (Isogai, 1994). However, the existence of two crystallographic phases for native cellulose, i.e. Iα and Iβ, was demonstrated more recently by Atalla and Vanderhart (1984) using ^{13}C solid state NMR. This finding was confirmed by other methods such as infrared spectroscopy (Sugiyama, Persson, & Chanzy, 1991a) and electron micro-diffraction (Sugiyama, Vuong, & Chanzy, 1991b). Electron micro-diffraction permitted the unit cells of each allomorph to be determined (Sugiyama et al., 1991b). In contrast to infrared spectroscopy and solid state NMR, X-ray powder scattering techniques (which are widely used to assess other polymorphic types and amount of crystallinity), are very difficult to optimise for the measurement of the Iα/Iβ ratio in native cellulose (Wada, Okano, & Sugiyama, 2001). The Iα form corresponds to a single-chain triclinic crystallographic symmetry, whereas Iβ is monoclinic and characterised by two parallel chains. Native cellulose is a mixture of these two forms, the ratio between Iα and Iβ depends on the source. It was also shown that the Iα phase was metastable and could be converted into the Iβ form by an hydrothermal treatment at 260 °C (Yamamoto, Horii, & Odani, 1989). Another variant among the different origins of cellulose is the proportion of surface chains (called the 'amorphous phase') compared to the 'in-core' crystalline material. This ratio, which defines the crystallinity of cellulose, is directly related to the lateral size of microfibrils and can be calculated via ^{13}C solid-state NMR (Newman, 1999; Newman & Hemmingson, 1990) or X-ray scattering using the Scherrer equation (Jakob, Fengel, Tschegg, & Fratzel, 1995; Jandura, Kokta, & Reidl, 2000). In addition to these analytical techniques, transmission electron microscopy (TEM) offers a direct view of the individual cellulose microfibrils via high-resolution lattice images.

In the present study, TEM, X-ray scattering, FT-IR spectroscopy and solid-state NMR techniques were used to investigate different levels of structure of new types of cellulose microfibrils extracted from maize and lemon. The polymorphic properties (Iα/Iβ ratio) were analysed by FT-IR and NMR spectroscopies. These methods have been used not only to detect and quantify the different cellulose polymorphs but also in combination with X-ray scattering to determine their crystallinity. Crystal size was determined by extrapolating the data from solid state NMR and X-ray scattering. Finally TEM was used to explore the global structure and the morphology of cellulose microfibrils. Moreover, the lattice imaging provided a good assessment of the homogeneity of microfibrils and sometimes made the direct measurement of microfibril size possible. Some dynamic information was also obtained from NMR measurements of the proton relaxation times in the rotating frame ($T_{1\rho}$). This parameter was measured for the various samples by ^{13}C CPMAS spectra in order to confirm our fitting strategy but also to validate the different crystallinity levels found by NMR.

These structural assessments were determined for cellulose microfibrils, extracted from two important agro-industrials waste: maize bran and lemon residues after pectin extraction. Besides the comparison of their structural characteristics, the two sources of cellulose were also compared for their physical behaviour after dispersion in an aqueous medium, since it was the intention to use the products for texturising food products.

2. Material

Maize bran and mixtures of maize microfibrils with carboxymethyl cellulose (CMC) were a gift from Amylum Nederland B.V. A mixture of MCC (Avicel) and CMC was purchased from FMC (US).

Hydrolyzed tunicin was obtained by 2.5N hydrochloric acid hydrolysis under reflux for 10 h.

The microfibrils were prepared from either lemon peel slurry which is a by-product of the industrial extraction of pectin (dry matter content ~10%) or from dry maize bran which was provided by Amylum Nederland B.V. After a bleaching/extraction stage with sodium hydroxide and hydrogen peroxide at high temperature, the slurry was neutralised using hydrochloric acid. It was filtered through a 250 μm sieve in order to eliminate the coarse fibres. The solid material was separated by centrifugation and washed with deionised water and separated again by centrifugation. Then, in some samples, hydrophilic gums such as CMC (Akucell AF 3085 from Akzo Nobel), xanthan gum or scleroglucan (from Degussa Texturant Systems) were added. The quantity of additional gums was 10% of the total dry solid content. The solid concentration was adjusted to 2% by adding water and the slurry was passed 3 times through a Guerin ALM2 homogeneiser at 250 bars. The microfibrils were dehydrated by mixing the suspension with isopropyl alcohol. The solid material was washed with pure isopropyl

Table 1
Characteristics of the different cellulose microfibrils studied

Name	Origin	Additive (10%)	Grinding	Others
Av/CMC	Wood (Avicel-FMC)	CMC	No	
AM/CMC	Maize (Amylum)	CMC	No	Sieved (500 μm)
L/CMC	Lemon	CMC	No	
L/CMC-G	Lemon	CMC	Yes	
L	Lemon	No	No	
L-G	Lemon	No	Yes	
M/CMC	Maize	CMC	No	
M/CMC-G	Maize	CMC	Yes	
M	Maize	No	No	
M-G	Maize	No	Yes	
L/SCL	Lemon	Scleroglucan	No	
L/XAN	Lemon	Xanthan	No	
L2/CMC	Lemon	CMC	No	
L2	Lemon	No	Blank	

alcohol, separated by filtration on a nylon cloth and pressed. The pressed material was dried in a fluidised bed drier. The dried product was either ground at 250 μm or sieved.

The main characteristics of the products studied are described in Table 1. Abbreviated names (first column) will be used for simplification.

3. Methods

3.1. ^{13}C solid state NMR (NMR)

NMR experiments were performed on a Bruker DMX-400 spectrometer operating at a ^{13}C frequency of 100.62 MHz and equipped with a double resonance H/X CP-MAS 4 mm probe. The MAS rate was fixed at 5000 Hz and each experiment was recorded at ambient temperature (294 ± 1 K). The Cross Polarisation pulse sequence used a 4.5 μs 90° proton pulse, a 1 ms contact time at 62.5 kHz and a 10 s recycle time for an acquisition time of 17 ms during which dipolar decoupling was applied. Typically 5120 scans were acquired for each spectrum. No line broadening was applied in order to perform the spectral fitting. Chemical shifts were determined by using the crystalline peak at 32.89 ppm of linear polyethylene as an internal standard.

The software used to fit each spectrum was based on the SIMPLEX method (dmfit2000- Massiot, Theile, & Germanus, 1994). Line types, full Lorentzian, full Gaussian or 50/50 Lorentzian/Gaussian were chosen depending on which gave the best fit. Generally, the Gaussian type lines fitted less-ordered components best whereas the Lorentzian lines were more suitable for highly crystalline components. When the fit did not work well with Lorentzion or Gaussian alone, a 50/50 mixture was chosen. Chemical shift, peak half-width and amplitude were then fitted with a fixed weight of Gaussian and Lorentzian functions. The highly crystalline tunicin was used as a model compound to calibrate the fit-strategy and the results found were in very good agreement with those reported in the literature (Heux, Dinand, & Vignon, 1999; Larsson, Westermark, & Iverson, 1995). In order to validate the fit, several spectra were recorded with varying parameters. This work was doubly interesting since it not only ensured that the fitting procedure had converged to a good result, but also measured the proton rotating-frame relaxation time $T_{1\rho}$ of each line-component. Measurements of the proton rotating-frame relaxation times $T_{1\rho}$ were achieved by varying the contact time (20 points between 200 ms and 30 ms) (Wu, Zhang, & Wu, 1988). A second series of spectra were recorded by adding a spin-lock (20 points between 200 and 30 ms at a power level of 62.5 KHz) of the proton magnetization before the contact time. For each series, the spectrum showing the maximum line intensity was fitted as described above, then for the others, by varying the spin-lock or the contact time, only the lines half-width and amplitude were fitted, and the chemical shifts were fixed.

The relative proportion of cellulose Iα and Iβ was determined by integrating the corresponding lines of the C1 signal (Horii, Hirai, & Kitamaru, 1987). The crystallinity degree was calculated from the area measured between 80 and 93 ppm of the C4 signal (minus the hemicellulose components) (Newman & Hemmingson, 1990). The lateral size of microfibrils was estimated according the Newman's method assuming a layer thickness of 0.57 nm (Newman, 1999).

3.2. Infrared spectroscopy (FT-IR)

Infrared measurements were performed on a Fourier Transform spectrometer (Bruker, Vector 22). The spectra were recorded in the transmission mode between 4000 and 400 cm^{-1} at 4 cm^{-1} intervals from KBr pellets (10% sample, w/w). A typical number of 200 scans were acquired for each spectrum. Baseline correction was achieved using the OPUS software (Bruker). The relative proportion of cellulose Iα and Iβ was determined by integrating the absorption bands near 750 and 710 cm^{-1} that are characteristic of Iα and Iβ allomorphs, respectively (Imai & Sugiyama, 1998; Sugiyama et al., 1991a). The percentage of Iβ allomorph was estimated by $\%I\beta = A_{710}/(A_{710} + A_{750})$ with A_{710} and A_{750}, being the integrated absorbance at about 710 and 750 cm^{-1}.

The degree of crystallinity was evaluated from the ratio of the absorption bands around 1280 and 1200 cm^{-1} (Hulleman, Van Hazendonk, & Van Dam, 1994). A decrease of the band at 1280 cm^{-1} is observed with decreasing crystallinity, while the band at 1200 cm^{-1} remains constant.

3.3. Wide angle X-ray scattering (WAXS)

Measurements were performed using a spectrometer equipped with a XRG 3000 generator (Inel Orléans, France)

working at 40 KV and 30 mA, a quartz monochromator ($\lambda = 0.15405$ nm) and a curve position sensitive detector (Inel CPS 120). Diffraction diagrams were recorded on 20 mg samples for 2 h in a transmission mode between 3 and 40° (2θ). All diagrams were normalized to the same total integrated area within this 2θ range.

The amount of crystallinity was determined using the method of Wakelin, Virgin, and Crystal (1959) with acid hydrolysed cellulose of tunicin and water reprecipitated cellulose from sulfuric acid solutions as crystalline and amorphous standards, respectively. The crystal sizes along and perpendicularly (a axis of the unit cell) to the chain axis were approximated from the half peak width of 004 ($2\theta \approx 34.5°$) and 200 ($2\theta \approx 22.2°$) bands, respectively. This was performed using the Scherrer equation: $D_{hkl} = K\lambda/\beta\cos\theta$, where β is the half peak width, λ the wavelength, D_{hkl} the average length of the diffracting domains normal to the family of planes (*hkl*), and K a constant usually taken as 0.9 for cellulose (Klug & Alexander, 1954). The crystalline part of the diagrams was first extracted by subtraction of the amorphous standard spectrum with a factor corresponding to the amount of amorphous regions determined by the Wakelin's method. The half peak widths were then determined after decomposition of the WAXS diagrams based upon the main reflexions known for cellulose Iβ and using the Peakfit software (Jandel Scientific). Fitted values obtained with Pearson 7 and Gaussian-Lorentzian profiles were compared.

3.4. Transmission electron microscopy (TEM)

Two percent (dry basis) suspensions of cellulose microfibrils were prepared in water by homogenisation at 15000 rpm for 2 min using a Polytron PT3000, then diluted ten times and homogenised again under the same conditions. Ten microliters of the suspension were deposited on a carbon coated grid and allowed to dry after blotting with a filter paper. Sample was then shadowed with Pt/Pd at an angle of 27° and observed using a Jeol 100S microscope at 80KV (magnification: 25000X and 50000X). The diameter of microfibrils was estimated from calibrated latex spheres (diameter 0.083 μm) added to the samples and shadowed.

3.5. Characterisation of the dispersion properties

As the presence of salts in the aqueous solvent is known to reduce the dispersing ability of cellulose, we chose to carry out the dispersion in milk. Thus, 2%wt suspensions were prepared by dispersing 6 g of cellulose into 394 g of semi-skimmed milk. The dispersion was made with a mechanical stirrer, Ikawerk RW20 equipped with an helix, at 2000 rpm for about 2 h. The suspension was then treated in an homogeniser, Guerin ALM2, at 250 bars in a recycling mode for 5 min, which is equivalent to about 12 passes.

After being dispersed the suspensions had a gel-like structure, the flow curves showed a strong shear thinning behaviour with a high yield value. The physical properties of the gel was characterised at room temperature with a Haake VT 550 viscometer equipped with a 6 blade vane, FL100, at 0.2 rpm. With this system we measured the torque as a function of time. An example of the mechanical profiles obtained is given in Fig. 1. The slope (mark 1) at low deformation (linear behaviour) gave the gel strength which is proportional to the elastic modulus. The maximum torque at the breaking point (mark 2) corresponded to the 'static' yield stress. Both these values are assumed to be proportional to the 'building' ability of the product and also to its dispersing ability. In order to simplify the analysis

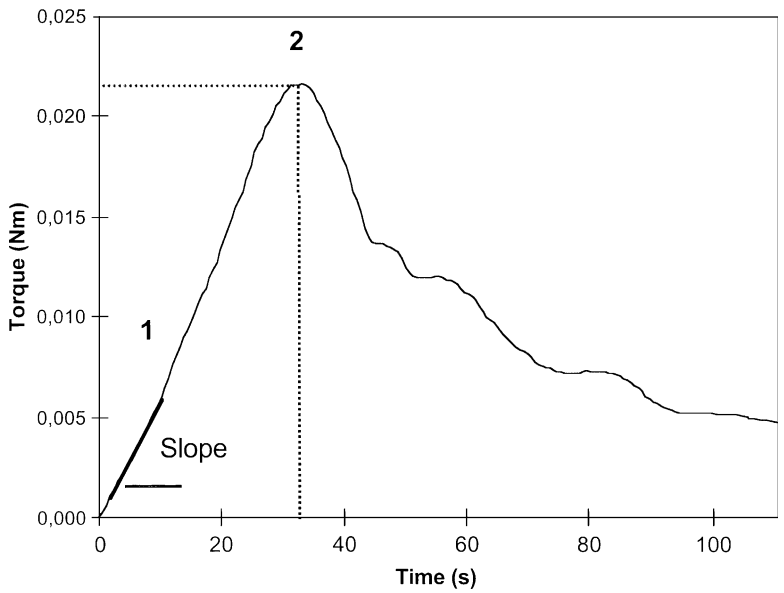

Fig. 1. Torque versus time obtained from the rheometer fitted with vane.

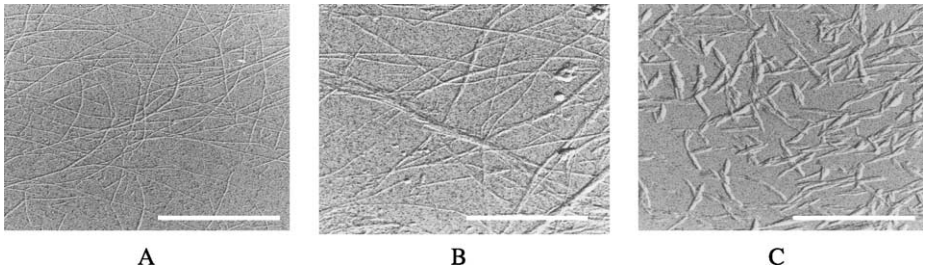

Fig. 2. Transmission electron micrographs of lemon (A), maize (B) and Avicel (C) cellulose microfibrils (bar = 1 μm).

and comparison of the various samples, only the torque value at the breaking point was recorded.

4. Results and discussion

4.1. Morphology

Fig. 2 shows electron micrographs of L and M by comparison to Av/CMC. Microfibrils from lemon and maize are less associated than Avicel which displays shorter microfibrils due to the hydrolysis used in its manufacture. The microfibrils bundles from lemon seem to be thinner than those from maize with an average thickness of apparently individual species of between 3 and 10 nm against 5 and 20 nm for maize, which indicates that they are more homogeneously dispersed than the maize samples.

4.2. Allomorphic type

Fig. 3 shows a ^{13}C NMR spectrum of highly crystalline cellulose obtained from acid hydrolyzed tunicin. This displays the well known four groups of resonances. On the upfield side of the spectrum, the region from 60 to 70 ppm is assigned to the C6 carbon, the more intense signals from 70 to 80 ppm are assigned to C2, C3 and C5 carbons, the next region from 80 to 90 ppm represents the resonance of C4, and finally the downfield signals belong to the C1 carbon. For this sample, which is known to contain 80–90% Iβ form, two signals at 105.7 ppm and 103.8 ppm compose the C1 resonances. Their assignment to the Iβ crystalline phase is now accepted and has been confirmed by several NMR studies (Atalla & Vanderhart, 1999; Larsson et al., 1995). To determine the allomorphic composition of the cellulose samples studied here, a spectral decomposition of C1 and C4 resonances was necessary due to their lower crystallinity, see Fig. 4 (for L and M samples) and Table 2 (for assignments of all samples). Only the C1 and C4 peaks were decomposed because they give all necessary informations for the determination of both cristallinity and Iα/Iβ ratio. Typical FT-IR spectra recorded for Av/CMC and M samples are shown in Fig. 5. In the 680–780 cm^{-1} domain (upper part), they show a major absorption band near 710 cm^{-1} for Av/CMC and two bands near 710 and 750 cm^{-1} for M sample which shows that Av/CMC consists mainly of Iβ allomorph, while M is a mixture of Iα and Iβ allomorphs. Blackwell, Vasko, and Koenig et al. (1970) have assigned the band near 750 cm^{-1} in *Valonia* to a CH_2 rocking mode of cellulose but this assignment is still questionable since no Raman absorption band exists in this region (Sugiyama et al., 1991a).

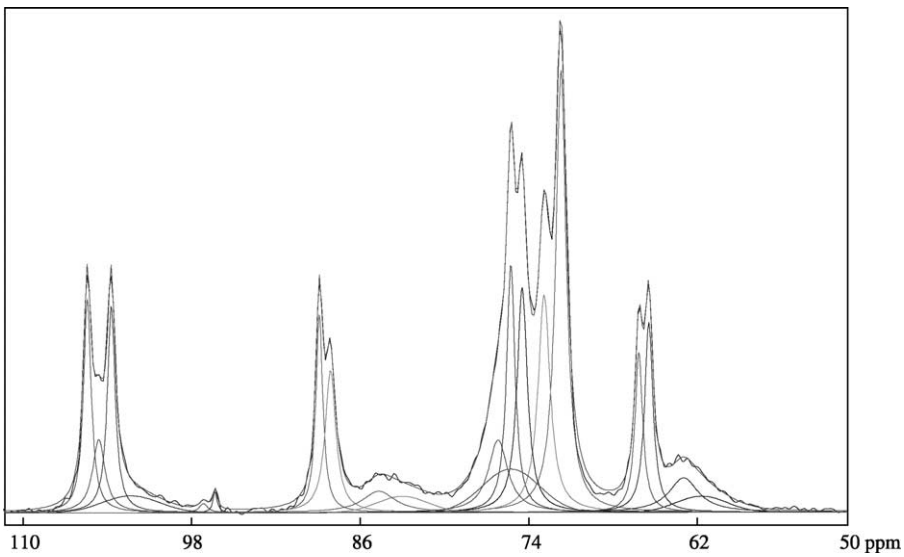

Fig. 3. Decomposition of the CP-MAS ^{13}C solid state NMR spectrum of tunicin cellulose.

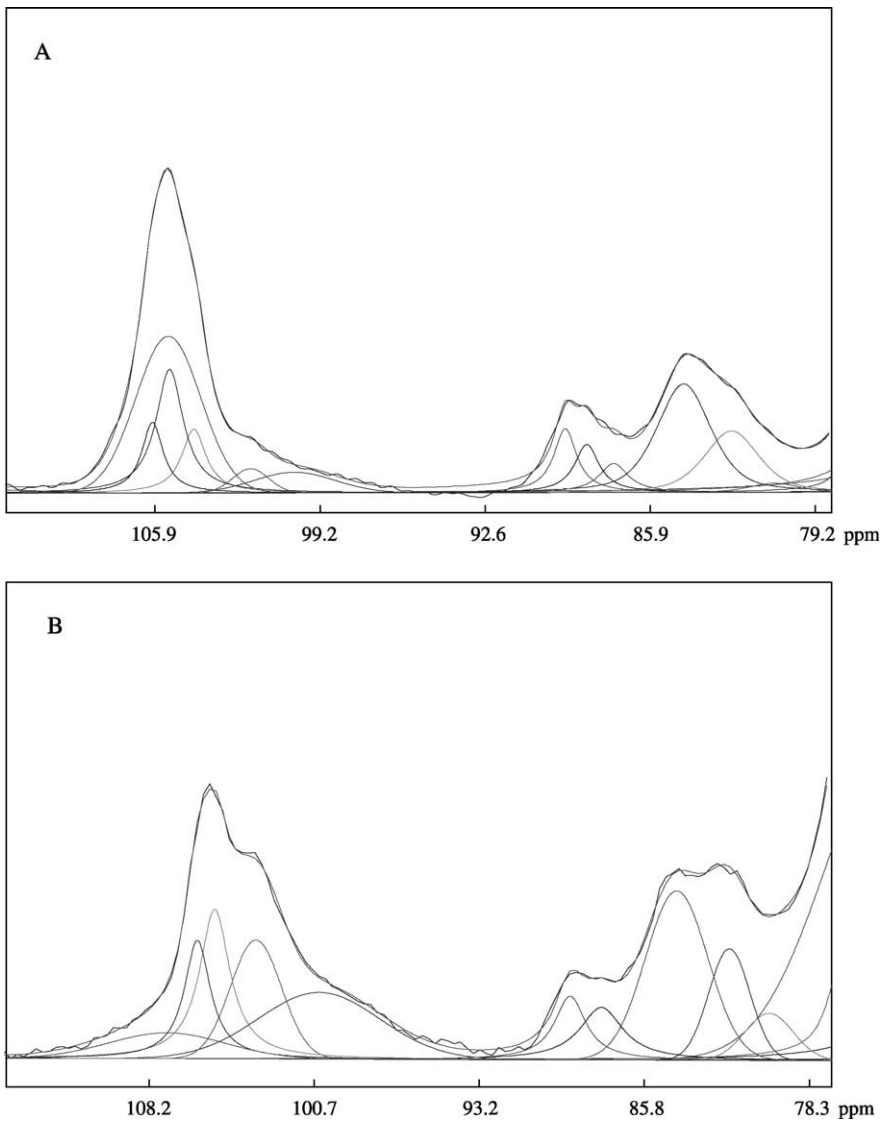

Fig. 4. Decomposition of the C1 and C4 signals of the CP-MAS ^{13}C solid state NMR spectra of lemon (A) and maize (B) celluloses.

Iα and Iβ proportions determined from both FT-IR and NMR spectra for the different studied samples are reported in Table 3. They depend strongly on the samples origin. Iβ varies from 52 to 94% by FT-IR and 51 to 76% by NMR. Results obtained for tunicin by NMR (76% Iβ) are in the same order of the literature reported values (Heux et al., 1999; Larsson et al., 1995). On the other samples, results obtained by FT-IR and solid-state NMR are comparable except for highly crystalline tunicin and avicel. This confirms that FT-IR determinations are tricky when %Iα (and therefore 750 cm^{-1} absorption) is weak. Moreover the pelleting technique used for samples preparation could induce a partial transformation from Iα to Iβ which could explain the higher %Iβ obtained by FT-IR comparatively to NMR. No important differences are observed between the lemon and maize celluloses which show Iβ values of 57 and 58% by FT-IR and 49 and 52% by NMR. Nevertheless, grinding has a strong effect especially for lemon cellulose since it increases %Iβ by 11%, this effect will be discussed later.

The presence of hemicelluloses was detected in each NMR spectrum with two typical C1 and C4 resonances, respectively at 98.33 ppm and 80.48–80.19 ppm for the lemon cellulose (L and L-G), and at 100.53 ppm and 80.12 ppm for the maize cellulose (M and M-G) (see Table 2). These lines contribute to the disordered region of cellulose and are tentatively assigned to C1 and C4 carbons of xylose or mannose. On the decomposed spectra of the maize cellulose, a line located at 107.42 ppm was also detected and tentatively assigned to some amorphous cellulose I. However, it has to be noted that this peak is in the chemical shift range of the C1 carbon of cellulose II (Hemmingson & Newman, 1995; Newman, Davies, & Harris, 1996).

Table 2
Assignment and $T_{1\rho}$ values of C1 and C4 carbons from solid state NMR spectra of lemon and maize celluloses (L, L-G, M and M-G), values in parentheses are the standard errors

Assignment		δ ppm	Intensity (%)	Line shape	$T_{1\rho}$ (ms)	Assignment		δ ppm	Intensity(%)	Line shape	$T_{1\rho}$ (ms)
Cellulose L											
C1	Iβ	105.99	0.51	L	11.73 (0.69)	C4	Iα	89.32	1.65	L	11.81 (0.45)
	Amorphous	105.40	8.17	G	8.47 (0.04)		Iα + Iβ	88.29	1.56	L	13.11 (0.02)
	Iα	105.28	1.91	L	9.72 (0.24)		Iβ	87.11	0.73	L	9.63 (1.49)
	Iβ	104.27	1.34	L	12.17 (1.09)		Fibril surfaces	84.66	4.65	L/G	10.74 (0.24)
	Amorphous	102.39	3.89	G	10.11 (0.73)		Fibril surfaces	82.73	4.02	L/G	10.64 (0.02)
	Hémicellulose	98.33	1.2	G	9.24 (0.88)		Hemicellulose	80.48	0.98	LG	6.04 (1.92)
Cellulose L-G											
C1	Iβ	105.99	0.78	L	12.43 (1.58)	C4	Iα	89.84	0.57	L	9.18 (0.64)
	Amorphous	105.40	6.41	G	7.13 (0.26)		Iα + Iβ	89.14	1.51	L	13.05 (0.09)
	Iα	105.28	1.85	L	12.79 (0.46)		Iβ	88.06	1.04	L	11.79 (0.71)
	Iβ	104.27	2.02	L	14.31 (1.61)		Fibril surfaces	84.48	3.91	L/G	8.55 (0.06)
	Amorphous	102.39	3.90	G	6.61 (0.11)		Fibril surfaces	82.45	4.61	L/G	8.29 (0.07)
	Hémicellulose	98.33	1.41	G	5.68 (0.71)		Hemicellulose	80.19	1.44	L/G	3.89 (0.47)
Cellulose M											
C1	Amorphous	107.42	1.55	G	2.59 (0.53)	C4	Iα	89.14	1.82	L	6.91 (0.42)
	Iβ	106.05	3.07	L	6.98 (0.07)		Iα + Iβ	87.72	1.91	L	7.97 (1.36)
	Iα + Iβ	105.26	3.86	L	11.01 (0.35)		Fibril surfaces	84.31	6.53	G	6.62 (0.22)
	Amorphous	103.39	3.95	G	3.94 (0.01)		Fibril surfaces	81.92	2.53	G	7.22 (0.93)
	Hémicellulose + Amorphous	100.53	4.83	G	4.68 (0.77)		Hemicellulose	80.12	1.64	G	4.29 (0.37)
Cellulose M-G											
C1	Amorphous	107.42	2.65	G	3.15 (0.02)	C4	Iα	89.14	1.60	L	7.46 (0.97)
	Iβ	106.05	3.41	L	6.50 (0.56)		Iα + Iβ	87.72	2.12	L	6.77 (0.16)
	Iα + Iβ	105.26	4.26	L	10.09 (0.56)		Fibril surfaces	84.31	6.47	G	6.37 (0.03)
	Amorphous	103.39	3.24	G	3.97 (0.04)		Fibril surfaces	81.92	2.80	G	6.69 (1.47)
	Hémicellulose + Amorphous	100.53	4.11	G	4.56 (0.65)		Hemicellulose	80.12	1.45	G	3.92 (0.74)

4.3. Crystallinity

Fig. 6 shows the WAXS diffractograms of hydrolysed tunicin, lemon (L) and maize (M) celluloses. All samples yielded cellulose I type diffraction diagrams, in contrast to the mixture of types I and IV proposed by Dinand et al. (1999) for sugar beet microfibrils. The light shift towards small angles of the (200) reflexion observed on less crystalline samples could be due to the increasing contribution of amorphous scattering to the total diffraction diagram. In fact, amorphous cellulose yields a broad scattering with a maximum of intensity at $2\theta = 21°$ (Cu Kα1 radiation). This was further confirmed by fine decomposition of the diagrams using the cellulose I most intense reflexions. The degrees of crystallinity estimated by WAXS, FT-IR and NMR for the different samples are reported in Table 4. Higher crystallinities were observed for hydrolysed tunicin (used as crystalline standard in WAXS data processing) and Avicel, which are hydrolysed during their preparation with a more or less complete elimination of amorphous or less-ordered zones. WAXS results indicate crystallinity for lemon cellulose (L and L2) varying between 51 and 55% whereas the values are lower for maize cellulose (AM-CMC and M) which contains 20–24% ordered zones. Similar values and/or tendencies are obtained from the FT-IR and NMR studies except for the lemon L sample which curiously seems to be characterised as less crystalline by these 2 techniques.

In addition to the direct measurement of crystallinity, ^{13}C CP-MAS NMR experiments are able to discriminate between mobile and rigid elements, that can be directly correlated with various levels of cristallinity. Indeed, slow motion (KHz range) of the polymer chain can be detected through the measurement of the proton rotating-frame

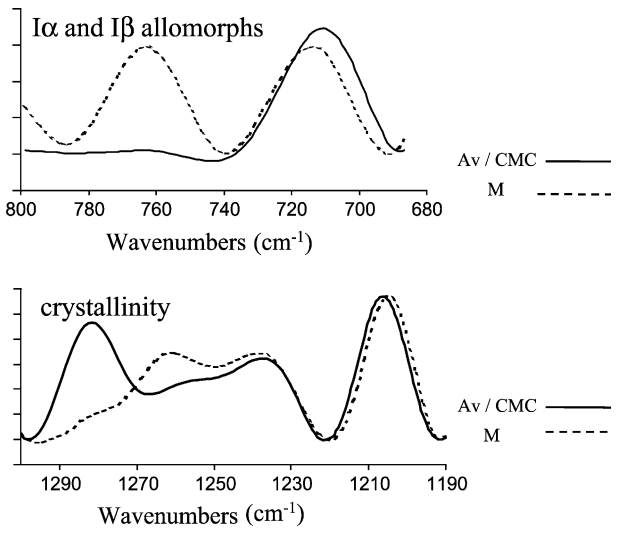

Fig. 5. FT-IR spectra of Avicel (AV/CMC) and maize (M) celluloses.

Table 3
Relative percentage of allomorphs Iα and Iβ determined by FT-IR and NMR

	FT-IR-% Iβ	NMR-% Iβ	NMR-% Iα
Tunicin	92	76	23
Av/CMC	94	68	32
AM/CMC	56	55	45
L	58	49	51
L-G	69	60	40
M	57	52	48
M-G	52	51	49

longitudinal relaxation times $T_{1\rho}$. This parameter is the most appropriate to probe the average mobility of differents domains of the cellulose microfibrils. Because the proton spectra show poor resolution, proton $T_{1\rho}$ are indirectly determined through their neighboring carbon by the cross-polarization technique. Values of the proton $T_{1\rho}$ relaxation times at the C1 and C4 carbon sites are reported in Table 2 for lemon (L, L-G) and maize (M and M-G) celluloses. For all samples, the proton $T_{1\rho}$ values measured for the crystalline parts (Iα + Iβ) are longer than the values of the less-ordered or amorphous zones. These results confirm the assignment of the different component bands. Indeed, the in-core crystalline material is more rigid and ordered, so corresponds to higher $T_{1\rho}$ relaxation times. In contrast the amorphous parts show a higher average mobility with lower $T_{1\rho}$ relaxation times. It must be noted that more than one peak assigned to the amorphous chains of cellulose has been resolved inside the C4 and C1

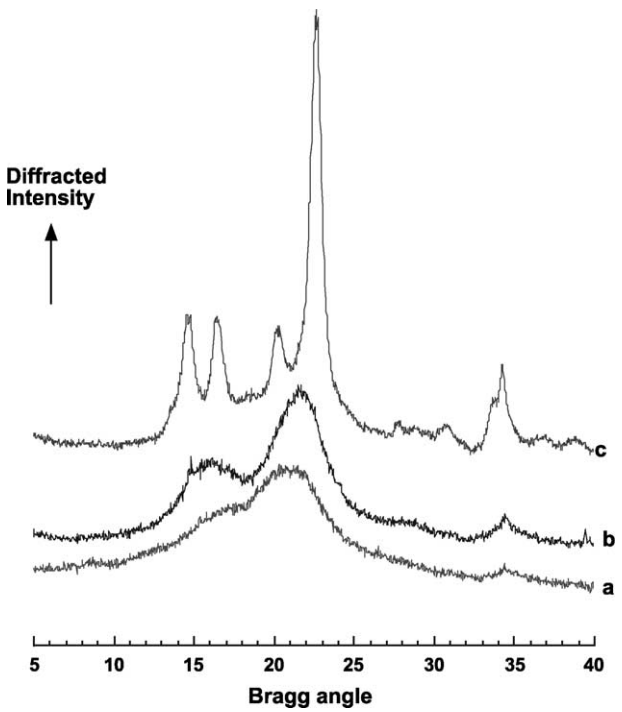

Fig. 6. X-ray diffractograms of (a) maize (M), (b) lemon(L) and (c) tunicin celluloses.

Table 4
Crystallinity degrees of cellulose microfibrils from different origins

Sample	% Crystallinity		
	WAXS	FT-IR	NMR
Tunicin	100	96	84
Av/CMC	66	54	57
Am/CMC	20	29	27
L	55	27	31
M	24	10	29
L2	51	27	nd

resonances. This splitting should arise from the different glycosidic linkage conformations present in these disordered parts of the microfibril (Ha et al., 1998). Based on solvent exchange experiments, Wickholm, Larsson, and Iverson (1998) have proposed assignment of these peaks to accessible and inaccessible fibril surfaces. Following the same point of view, Rowland and Howley (1988) considered various categories of disorder on the crystallite surfaces. Therefore some chains might interact with chains on another surface resulting in aggregates of coaxial fibrils, and other might be exposed to the surrounding medium. Another model can be proposed, where some disordered chains of cellulose are located in the interior of microfibrils, between ordered crystalline chains. The intersticial amorphous part could arise from the para-crystalline cellulose proposed by Larsson, Wickholm, and Iverson (1997) and are probably produced by distortion extensions into the fibril interior.

The $T_{1\rho}$ values of the lemon cellulose L and L-G are longer that the maize cellulose ones. A simple interpretation of these results could conclude that the lemon cellulose is more crystalline. This is consistent with the relatively high degree of crystallinity (around 50%) determined for the lemon cellulose by X-ray diffraction. However, the crystallinities determined by ^{13}C CP-MAS NMR and FT-IR are the same for lemon and maize. No explanation for this apparent discrepancy has been found.

4.4. Crystal size in microfibrils

Microfibrils lateral size can be directly calculated from the crystallinity ratios determined by ^{13}C CP-MAS NMR (Newman & Hemmingson, 1990). The Newman's model is based on the assumption of a squared cross-section with sides composed of n cellulose chains placed on the monoclinic crystal lattice (Sugiyama et al., 1991b). We estimated the microfibrils lateral size L assuming a square cross-section with sides $L = 0.57.n$, the value 0.57 nm corresponding to the average d-spacing calculated from the interchains distance in the two pairs of faces of the monoclinic lattice (Sugiyama et al., 1991b). Some estimations were also drawn from the 200 scattering peak width ($2\theta \approx 22.2°$), using the Scherrer equation after decomposition of WAXS diagrams. Finally some evaluations of

the chain length involved in the crystal regions were made from the 004 reflexion ($2\theta \approx 34.6°$) in the same WAXS diagrams.

The cellulose microfibrils lateral sizes reported in Table 5 vary from 13.6 and 9.1 nm for tunicin to around 2.5 and 3.5 nm for the lemon and maize cellulose, respectively from NMR and WAXS data. Between the two extremes, Avicel presents a lateral size of 4.6 nm by NMR against 5.5 by WAXS. Except for tunicin which is almost purely crystalline, the values determined by NMR are slightly smaller than those obtained by diffraction. Moreover, the NMR values are smaller than those found for sugar beet (Heux et al., 1999). These differences observed between NMR and WAXS data can be a consequence of the hypotheses used in the calculation. The lateral size depends on the amount of crystallinity. Indeed, the more crystalline the cellulose is, the larger the microfibrils lateral size is. In the hypotheses used, amorphous regions of samples are assumed to be limited to the surface of microfibrils, which is probably true for hydrolysed tunicin but not for poorly crystalline samples such as those prepared from maize or lemon. In such substrates, whose the crystallinity ranges between 20 and 55%, some amorphous and crystalline regions probably alternate along the microfibril. Secondly, a square cross-section was used in the calculations. Such a model was already used by Heux et al. (1999) for sugar beet microfibrils and assumed pure Iβ allomorph. On the other hand, values determined by TEM are three times higher, even for samples which appear to be single microfibrils, which might suggest that in fact they are composed of several individual microfibrils. Finally, the 004 reflexion ($2\theta \approx 35°$) was used to approach the length of the crystalline parts (i.e. following the polymer chains axis) using the Scherrer equation. The calculated values are given in Table 5, they are higher for lemon (from 5.5 to 8) than for maize (2.1–4.6 nm) which can also be associated with the lower crystallinity of the latter.

Table 5
Crystallite sizes measured by X-ray diffraction from the 020 and 004 reflexions and by solid-state NMR

Sample	Crystal lateral size (D200 X-ray)	Crystal lateral size (NMR)	Crystal length (D004 X-ray)
Tunicine	9.1	13.6	nd
Av/CMC	5.5	4.6	nd
AM/CMC	3.3	2.4	nd
L/CMC	3.5	nd	6.2
L	3.5	2.6	6.6
L-G	2.8	2.4	5.6
M/CMC	nd	nd	3.4
M	3.5	2.5	2.3
L-SCL	nd	nd	4.9
L-XAN	nd	nd	7.3
L2-CMC	nd	nd	8.3
L2	3.5	nd	7.2

4.5. Effect of grinding

Fig. 7 displays the WAXS diffractograms of the lemon cellulose microfibrils with and without grinding (L and L-G samples). The global crystallinity decreases after grinding from 55% to 34% as shown in the Table 6. This result, confirmed on four different batches of lemon cellulose microfibrils, is also observed by NMR but at a lower scale, a decrease of only 4% being determined. The L-G cellulose contains more desordered parts and consequently the crystallite lateral size decreases, with values decreasing from 2.6 nm for L to 2.4 nm for L-G (Table 5). This was also found from WAXS with a size decrease from 3.5 to 2.8 nm. No crystallinity changes were observed on maize samples M and M-G.

The proton relaxation times $T_{1\rho}$ values reported in Table 2, show the same tendency as the crystallinity degree. Indeed, the lemon cellulose $T_{1\rho}$ values are affected by grinding as the amorphous and fibrils surfaces results show. A decrease from 1 to 3.5 ms is observed between the less-ordered microfibrils zones for the two samples, L and L-G. The hemicellulose components undergo similar effects since they have higher average mobilities, which is compatible with their presence in the outside disordered parts of the cellulose microfibrils. In addition, the in-core crystalline part of lemon cellulose shows an increase of the Iβ phase at the expense of the Iα ones. Consequently, the mechanical grinding technique seems to affect the lemon microfibrils surfaces resulting in a reduction in crystallinity and a conversion of 11% of the Iα phase into the Iβ form. The higher susceptibility of lemon samples could be explained by their relatively high crystallinity and crystal size which make them more rigid and breakable. Changes in the Iα/Iβ ratio under mechanical treatment has been already observed (Dufresne et al., 2000) and confirms the more limited stability of the Iα form which is more prone to be degraded by enzymes (Hayashi, Sugiyama, Okano, & Ishihara, 1998) and which can be converted into the Iβ form by different

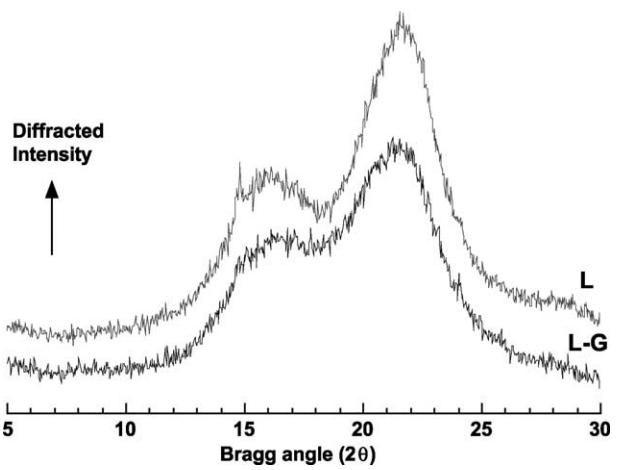

Fig. 7. Effect of grinding on the crystallinity of lemon cellulose microfibrils.

Table 6
Effect of grinding on the crystallinity of lemon and maize microfibrils

Name	Origin	Additive (10%)	Grinding	Crystallinity %
L/CMC	Lemon	CMC	No	52
L/CMC-G	Lemon	CMC	Yes	33
L	Lemon	No	No	55
L-G	Lemon	No	Yes	34
M/CMC	Maize	CMC	No	26
M/CMC-G	Maize	CMC	Yes	24
M	Maize	No	No	24
M-G	Maize	No	Yes	24
L2/CMC	Lemon	CMC	No	55
L2	Lemon	Blank	No	52

treatments and especially heat treatments (Sugiyama et al., 1991a).

Addition of CMC to lemon and maize microfibrils does not change their behavior during grinding and the changes in crystallinity are the same as for pure products (Table 6). The effects of scleroglucan or xanthan addition are more difficult to understand with a more or less pronounced decrease in the crystallinity observed on lemon microfibrils even after subtraction of normalized additive diffraction diagrams. Further work is necessary to check if these results are due to a real effect of the added material or to a non-additivity of the diffraction diagrams.

4.6. Dispersion and building properties

The values of the measured torques are given in the Table 7. The CMC activated lemon cellulose gave the best results with a torque value of 3.37 mN m as compared with 1.96 mN m for the non-activated lemon cellulose. Nevertheless, in a 'fresh state' i.e. just before being dried, the lemon cellulose dispersion activated with CMC had a torque of about 6 mN m. This means that, even if the salt content was not exactly the same in milk as in the process fluid, the full physical properties of the gel were not recovered after drying. Drying causes incomplete dispersal of the product. The effect of CMC was also observed for the cellulose from maize bran. The addition of scleroglucan and xanthan had no effect. Even in the presence of CMC, the grinding stage made the product more difficult to disperse and the torque value was reduced to 1.99 mM.m for ground lemon cellulose. With respect to the various sources, lemon microfibrils dispersed significantly better than maize in both cases with or without CMC. The wood cellulose which was activated with CMC was very difficult to disperse under these conditions.

Table 7
Dispersion and texturising properties: torques at the breaking point for the various samples

Samples (mN m)	Additive (10%)	Grinding	Torque(mN m)
Av/CMC	CMC	No	0.74
AM/CMC	CMC	No	2.93
L	No	No	1.96
L/CMC	CMC	No	3.37
L/CMC-G	CMC	Yes	1.99
L/SCL	Scleroglucan	No	1.86
L/XAN	Xanthan	No	1.99
M	No	No	0.67
M/CMC	CMC	No	2.19

Although celluloses from lemon and maize are different to MCC in terms of structure, the analysis of the results is based on the functional model of MCC (Nussinovitch, 1997). In this model, the physical transformation of the aqueous medium is due to the fact that cellulose crystallites are able to disperse in an aqueous medium and then to establish a network. The physical property which is measured here is therefore connected to both the dispersion ability of the product and the ability to establish the structure of the network. For highly crystalline celluloses, less bonds are necessary to set up a network since crystallites are already connected. Thus, the product is prone to form a strong network, conferring a high yield value to the dispersed suspensions. It is inferred that lemon microfibrils give higher torques than maize since citrus microfibrils are thinner and more crystalline than those from maize. In lemon and maize microfibrils, the crystalline zones are covered by amorphous surface chains and probably by hemicelluloses (see above). Moreover, it is likely that some other disordered chains alternate within the microfibrils which are long and thin and probably rather flexible. Consequently, less aggregation of the crystallites arises during drying. This may explain why dispersion would be easier with lemon and maize cellulose than with wood cellulose.

The grinding effect may be explained by the degradation of crystallites which results in a decrease of the percentage of crystallinity. This could reduce the ability to produce a network and to lower the yield value of the suspension. The effect of CMC (which has a backbone similar to cellulose in comparison with other gums) is explained by its adsorption onto the surface of the microfibrils. The action is similar to hemicelluloses in avoiding collapse during the drying stage and introducing more hydrophilic regions.

5. Conclusions

An extensive study of the structural parameters of cellulose microfibrils extracted from lemon and maize was performed for the first time. The complementary techniques used (WAXS, NMR, TEM and FT-IR especially) was efficient to assess the different levels of structure (morphology, amount of crystallinity, crystal size, allomorphic type…) and the effect of processing. Some of the measured characteristics on lemon samples

were very close to those described on sugar beet microfibrils by Dinand et al. (1996) with comparable crystallinity (around 50%) but a slightly smaller crystal size drawn from NMR data. These substrates could represent an interesting alternative for valorisation of by-products of pectin industry and agriculture, respectively, and preliminary trials of their potential texturising properties in liquid systems were carried out. The structural characteristics observed are very different for the two sources, lemon giving higher cristallinity, crystal size and microfibril diameter and also better texturising properties. Moreover, these properties can be reached without addition of hydrophilic gums such as CMC in contrast to maize microfibrils. Nevertheless, these properties are highly sensitive to grinding.

References

Atalla, R. H. (1999). *Celluloses* (*Vol. 3*). *Comprehensive natural products chemistry*, Elsevier Science Ltd, p. 529.

Atalla, R. H., & Vanderhart, D. L. (1984). Native cellulose: A composite of two distinct crystalline forms. *Science*, *223*, 283–287.

Atalla, R. H., & Vanderhart, D. L. (1999). The role of solid-state ^{13}C NMR spectroscopy in studies of the nature of native celluloses. *Solid State NMR*, *15*, 1–19.

Blackwell, J., Vasko, P., & Koenig, J. (1970). Infrared and Raman spectra of the cellulose from the cell wall of *Valonia ventricosa*. *Journal of Applied Physics*, *41*, 4375–4379.

Carpita, N. C., & Gibeaut, D. M. (1993). Structural models of primary cell walls in flowering plants: Consistency of molecular structure with the physical properties of the walls during growth. *Plant Journal*, *3*, 1–30.

Davis, W. E., Barry, A. J., Peterson, F. C., & King, A. J. (1943). X-ray studies of reactions of cellulose in non-aqueous systems. II. Interaction of cellulose and primary amines. *Journal of the American Chemical Society*, *65*, 1294–1300.

Dinand, E., Chanzy, H., & Vignon, M. R. (1996). Parenchymal cell cellulose from sugar beet pulp: Preparation and properties. *Cellulose*, *3*, 183–188.

Dinand, E., Chanzy, H., & Vignon, M. R. (1999). Suspensions of cellulose microfibrils from sugar beet pulp. *Food Hydrocolloids*, *13*, 275–283.

Dufresne, A., Cavaillé, J.-Y., & Vignon, M. (1997). Mechanical behavior of sheets prepared from sugar beet cellulose microfibrils. *Journal of Applied Polymer Science*, *64*, 1185–1194.

Dufresne, A., Dupeyre, D., & Vignon, M. (2000). Cellulose microfibrils from potato tuber cells: Processing and characterization of starch-cellulose microfibrils composites. *Journal of Applied Polymer Science*, *76*, 2080–2092.

Ginley, E. J., & Tauson, D. C. (1990). Application of microcrystalline cellulose. In G. O. Philips, P. A. Williams, & D. J. Wedlock (Eds.), (*Vol. 5*) (pp. 405–414). *Gums and stabilisers for the food industry*, Oxford: IRL Press.

Ha, M. A., Apperley, D. C., Evans, B. W., Huxham, M. I., Jardine, W. G., Viëtor, R. J., Reis, D., Vian, B., & Jarvis, M. C. (1998). Fine structure in cellulose microfibrils: NMR evidence from onion and quince. *Plant Journal*, *16*, 183–190.

Hayashi, N., Sugiyama, J., Okano, T., & Ishihara, M. (1998). Selective degradation of the cellulose Iα component in *Cladophora* cellulose with *Trichoderma viride* cellulase. *Carbohydrate Research*, *305*, 109–116.

Hemmingson, J. A., & Newman, R. H. (1995). Changes in molecular ordering associated with alkali treatment and vacuum drying of cellulose. *Cellulose*, *2*, 71–82.

Hess, K., & Kiessig, H. (1941). Zur kenntnis der hochtemperatur. Modifikation der cellulose (cellulose IV). *Zeitschrift fuer Physikalische Chemie*, *49*, 235–239.

Heux, L., Dinand, E., & Vignon, M. R. (1999). Structural aspects in ultrathin cellulose microfibrils followed by ^{13}C CP-MAS NMR. *Carbohydrate Polymers*, *40*, 115–124.

Horii, F. (2000). *Structure of cellulose: Recent developments in its characterization* (Second ed.). *Wood and cellulosic chemistry*, New York: Marcel Dekker, Inc, p. 83.

Horii, F., Hirai, A., & Kitamaru, R. (1987). CP/MAS ^{13}C NMR spectra of the crystalline components of native celluloses. *Macromolecules*, *20*, 2117–2120.

Hulleman, S. H. D., Van Hazendonk, J. M., & Van Dam, J. E. G. (1994). Determination of crystallinity in native cellulose from higher plants with diffuse reflectance fourier-transform infrared spectroscopy. *Carbohydrate Research*, *261*, 163–172.

Imai, T., & Sugiyama, J. (1998). Nanodomains of Iα and Iβ cellulose in algal microfibrils. *Macromolecules*, *31*, 6275–6279.

Isogai, A. (1994). *Allomorphs of cellulose and other polysaccharides*. *Cellulosic polymers, blend and composites*, Munich: Hanser Publisher, pp. 1–24.

Jakob, H. F., Fengel, D., Tschegg, S. E., & Fratzl, P. (1995). The elementary cellulose fibril in *Picea abies*: Comparison of transmission electron microscopy, small-angle X-ray scattering, and wide-angle X-ray scattering results. *Macromolecules*, *28*, 8782–8787.

Jandura, P., Kokta, B. V., & Riedl, B. (2000). Fibrous long-chain organic acid cellulose esters and their characterization by diffuse reflectance FTIR spectroscopy, solid-state CP/MAS ^{13}C NMR and X-ray diffraction. *Journal of Applied Polymer Science*, *78*, 1354–1365.

Klug, H., & Alexander, L. (1954). *X-ray diffraction procedures for polycrystalline and amorphous materials*. New York: John Wiley Interscience, pp. 491–538.

Larsson, P. T., Westermark, U., & Iversen, T. (1995). Determination of the cellulose Iα allomorph content in tunicate cellulose by CP/MAS ^{13}C-NMR spectroscopy. *Carbohydrate Research*, *278*, 339–343.

Larsson, P. T., Wickholm, K., & Iversen, T. (1997). A CP/MAS ^{13}C NMRinvestigation of molecular ordering in celluloses. *Carbohydrate Research*, *302*, 19–25.

Massiot, D., Thiele, H., & Germanus, A. (1994). WinFit: A Windows-based program for lineshape analysis. *Bruker Report*, *140*, 43–46.

Newman, R. H. (1999). Estimation of the lateral dimensions of cellulose crystallites using ^{13}C NMR signal strengths. *Solid State NMR*, *15*, 21–29.

Newman, R. H., Davies, L. M., & Harris, P. J. (1996). Solid state ^{13}C nuclear magnetic resonance characterization of cellulose in the cell walls of *Arabidopsis thaliana* leaves. *Plant Physiology*, *111*, 475–485.

Newman, R. H., & Hemmingson, J. A. (1990). Determination of the degree of cellulose crystallinity in wood by carbon-13 nuclear magnetic resonance spectroscopy. *Holzforschung*, *44*, 351–355.

Nussinovitch, A. (1997). *Cellulose derivatives*. *Hydrocolloid applications*, London: Blackie Academic and Professional, pp. 105–124.

Petitpas, T., Oberlin, M., & Mering, J. (1963). Confirmation d'une hypothèse de P.H. Hermans: Chaîne de la cellulose II. *Journal of Polymer Science, C*, *2*, 423–427.

Rowland, S. P., & Howley, P. S. (1988). Structure in "amorphous regions", accessible segments of fibrils of the cotton fiber. *Textile Research Journal*, *58*, 96–101.

Salmon, S., & Hudson, S. M. (1997). Crystal morphology, biosynthesis and physical assembly of cellulose, chitin and chitosan. *Reviews in Macromolecular Chemical Physics*, *C37*, 199–276.

Sarko, A. (1978). What is the crystalline structure of cellulose? *Tappi*, *61*, 59–61.

Sarko, A., & Mugli, J. (1974). Packing analysis of carbohydrates and polysaccharides. III. *Valonia* cellulose and cellulose II. *Macromolecules*, *7*, 486–494.

Sugiyama, J., Persson, J., & Chanzy, H. (1991a). Combined infrared and electron diffraction study of the polymorphism of native celluloses. *Macromolecules*, *24*, 2461–2466.

Sugiyama, J., Vuong, R., & Chanzy, H. (1991b). Electron diffraction study on the two crystalline pahses occuring in native cellulose from an algal cell wall. *Macromolecules*, *24*, 4168–4175.

Wada, M., Okano, K., & Sugiyama, J. (2001). Allomorphs of native crystalline cellulose I evaluated by two equatorial d-spacings. *Journal of Wood Science*, *47*, 124–128.

Wakelin, J. H., Virgin, H. S., & Crystal, E. (1959). Development and comparison of two X-ray methods for determining the crystallinity of cotton cellulose. *Journal of Applied physics*, *30*, 1654–1662.

Wickholm, K., Larsson, P. T., & Iversen, T. (1998). Assignment of non-crystalline forms in cellulose I by CP/MAS ^{13}C NMR spectroscopy. *Carbohydrate Research*, *312*, 123–129.

Wu, X., Zhang, S., & Wu, X. (1988). Two-stage feature of Hartmann-Hahn cross relaxation in magic-angle sample spinning. *Physical Review B*, *37*, 9827–9829.

Yamamoto, H., Horii, F., & Odani, H. (1989). Structural changes of native cellulose crystals induced by annealing in aqueous alkaline and acid solutions at high temperatures. *Macromolecules*, *22*, 4130–4132.